GEVHER NESIBE JOURNAL OF MEDICAL & HEALTH SCIENCES | ISSN 2717-7394

Arrival Date: 05.05.2026 | Published Date: 14.06.2026 | Vol: 11, Issue: 2 | pp: 167-180 | Doi Number: https://doi.org/10.5281/zenodo.20701652

A FUNCTIONAL AND RELATIONAL INVESTIGATION OF DIFFERENCES IN BRAIN REGIONS BASED ON GRAPH ANALYSIS METRICS IN CHILDREN WITH DYSLEXIA

DİSLEKSİLİ ÇOCUKLARDA GRAF ANALİZİ METRİKLERİNE DAYALI BEYİN BÖLGELERİNDEKİ FARKLARIN FONKSİYONEL VE İLİŞKİSEL ARAŞTIRILMASI

Gizem Rüveyda SAĞIR [1], Semra İÇER [2], Şerife GENGEÇ BENLİ [2], Esra DEMİRCİ [3], Zehra Filiz KARAMAN [4]

[1] Erciyes University, Graduate School of Natural and Applied Sciences, Department of Biomedical Engineering, Kayseri, Türkiye.
[2] Erciyes University, Engineering Faculty, Department of Biomedical Engineering, Kayseri, Türkiye.
[3] Erciyes University, Faculty of Medicine, Department of Child and Adolescent Psychiatry, Kayseri, Türkiye.
[4] Erciyes University, Faculty of Medicine, Department of Pediatric Radiology, Kayseri, Türkiye.

ABSTRACT

Objective: Developmental dyslexia is a neurodevelopmental disorder that begins in childhood and is characterized by persistent impairments in reading and writing abilities, despite adequate intellectual functioning and educational opportunities. Investigating the topological properties of functional brain networks in dyslexia can provide valuable insights into its underlying neural mechanisms.

Method: In this study, three groups were compared: children with primary dyslexia diagnosis (Dys, n=25), children with dyslexia who received education (EDys, n=24), and healthy children (HC, n=25). Functional magnetic resonance imaging (fMRI) data were acquired from all participants during both resting-state and continuous reading tasks. The data were preprocessed using FSL software, and graph-theoretical network analysis was conducted using the GRETNA toolbox. Nodal-level graph metrics, including degree centrality, betweenness centrality, nodal efficiency, nodal local efficiency, and nodal clustering coefficient, were computed. Functional differences between the resting state and the reading task within each group were examined and correlation analysis between the metrics was performed both across groups and within each group for both conditions.

Results: In the graph analysis, the Dys group exhibited significantly higher network metric specifically degree centrality and nodal efficiency during the reading task in the right superior frontal gyrus and right superior parietal lobule, whereas these metrics were higher during the resting state in the bilateral rectus and right cerebellum ($p < 0.05$). For the EDys group, an increase was sated in betweenness centrality and degree centrality metrics during the resting state in the left angular gyrus and right superior temporal pole, and during the reading task in the left inferior occipital gyrus ($p < 0.05$). In the HC group, betweenness centrality and nodal clustering coefficient metrics in the left fusiform gyrus, as well as nodal local efficiency and nodal clustering coefficient metrics in the right calcarine cortex, were found to be significantly higher during the resting state compared to the reading task ($p < 0.05$). Correlation results revealed that during the reading task, the EDys and HC groups exhibited more abundant and significant interactions ($r > 0.7$) among metrics compared to the Dys group.

Conclusion: These findings indicate a compensatory hyper-activation in frontal and parietal regions during reading in primary dyslexic children, and a topological reorganization of network metrics in visual-processing areas such as the left inferior occipital gyrus in educated dyslexic children. Our results provide crucial topological evidence regarding the neural mechanisms of dyslexia and special education-induced neuroplasticity.

Keywords: Dyslexia, Correlation Analysis, Graph Analysis, Reading-task, Special Education

ÖZET

Amaç: Gelişimsel disleksi, zekâ düzeyi ve eğitim olanakları yeterli olmasına rağmen okuma ve yazma becerilerinde kalıcı bozulmalarla karakterize edilen, çocuklukta başlayan nörogelişimsel bir bozukluktur. Dislekside, işlevsel beyin ağlarının topolojik özelliklerinin incelenmesi, disleksinin nöral temellerinin daha iyi anlaşılmasına katkı sağlayabilir.

Yöntem: Bu çalışmada, ilk kez disleksi tanısı almış çocuklar (Dys, n=25), özel eğitim desteği almış disleksili çocuklar (EDys, n=24) ve sağlıklı kontrol çocuklarından (HC, n=25) oluşan üç grup karşılaştırılmıştır. Tüm katılımcılardan dinlenme durumu ve sürekli okuma görevi sırasında fonksiyonel manyetik rezonans görüntüleme (fMRI) verileri toplanmıştır. fMRI verileri, FSL yazılımı kullanılarak önişlemden geçirilmiş ve ardından GRETNA yazılımı aracılığıyla graph ağ analizi gerçekleştirilmiştir. Analizde, derece merkeziliği, aradalık merkeziliği, düğüm verimliliği, yerel düğüm verimliliği ve düğüm kümeleme katsayısı gibi temel nodal metrikler hesaplanmıştır. Her grubun kendi içinde dinlenme durumu ile okuma görevi arasındaki fonksiyonel farklar incelenmiş, ayrıca her iki durum için hem gruplar arası hem de her grubun kendi içindeki metrikler arası korelasyon analizi yapılmıştır.

Bulgular: Graph analizinde Dys grubunda okuma görevinde sağ superior frontal girus ve sağ superior parietal lobda; dinlenme durumunda ise sol/sağ rectus ve sağ beyincikte derece merkeziliği ve düğüm verimliliği, ağ metrikleri daha yüksek bulunmuştur ($p<0.05$). EDys grubunda aradalık merkeziliği ve derece merkeziliği metriklerinde, dinlenme durumunda sol angular girus ve sağ superior temporal polde; okuma görevinde ise sol inferior oksipital girusta artış saptanmıştır ($p<0.05$). HC grubunda dinlenme durumunda aradalık merkeziliği ve düğüm kümeleme katsayısı metriklerinde sol fusiform girus, düğüm yerel verimliliği ve düğüm kümeleme katsayısı metriklerinde ise sağ kalkarin korteks okuma görevine göre daha yüksek çıkmıştır

(p<0.05). Korelasyon sonuçları, okuma görevi esnasında EDys ve HC gruplarının metrikler arasında Dys grubuna kıyasla daha yoğun ve anlamlı ilişkiler (r>0.7) sergilediğini göstermiştir.
Sonuç: Bu bulgular, ilk kez tanı alan disleksili çocuklarda okuma esnasında frontal ve parietal bölgelerde telafi edici bir aşırı aktivasyon olduğunu, özel eğitim alan çocuklarda ise sol inferior oksipital girus gibi görsel-işlemsel alanlarda ağ metriklerinin yeniden organize olduğunu göstermektedir. Sonuçlarımız, disleksinin nöral mekanizmalarına ve özel eğitimin tetiklediği nöroplastisiteye dair önemli topolojik kanıtlar sunmaktadır.
Anahtar Kelimeler: Disleksi, Graf Analizi, Korelasyon analizi, Okuma Görevi, Özel Eğitim,

Corresponding Author: Şerife GENGEÇ BENLİ, Erciyes University, Engineering Faculty, Department of Biomedical Engineering, Kayseri, Türkiye. **E-mail:** serifegengec@gmail.com

Cite this article: SAĞIR, R.G., İÇER, S., BENLİ, G.Ş., DEMİRCİ, E.İ., KARAMAN, F.Z. (2026). A Functional and Relational Investigation of Differences In Brain Regions Based on Graph Analysis Metrics in Children With Dyslexia. Gevher Nesibe Journal of Medical & Health Science. 11(2), 167 DOI: https://doi.org/10.5281/zenodo.20701652

INTRODUCTION

Developmental dyslexia is a common learning disorder associated with a specific difficulty in reading despite intelligence, environment, or educational opportunities, and it affects 5–10% of the population worldwide (Lyon, Shaywitz, & Shaywitz, 2003; Norton, Beach, & Gabrieli, 2015). Studies on developmental dyslexia have revealed various impairments in the brain networks involved in reading (Bullmore & Sporns, 2009). Although certain brain regions have been successfully associated with literacy acquisition, a more holistic approach may be necessary to understand a highly complex cognitive function like reading (Bullmore & Sporns, 2009). In dyslexia, in order to reveal the underlying causes of reading disorder, differences in brain activity during rest and task conditions have been examined using various neuroimaging techniques in the literature. Functional imaging studies have consistently reported that children with dyslexia show less or reduced activation in the parieto-temporal regions of the brain compared to typically developing children (Boets et al., 2013; Vandermosten et al., 2012). Additionally, they have suggested that impaired functional relationships between brain regions in reading areas may be the cause of dyslexia (Boets et al., 2013; Vandermosten et al., 2012).

Traditional fMRI analysis methods may not always provide a complete understanding of the neurological foundations of dyslexia. Although some studies on dyslexia have examined functional connectivity (van der Mark et al., 2011; Vogel et al., 2012), all of these studies have focused on interactions between specific, predefined brain regions. However, beyond these region-based approaches, there are also network-based methods that offer a different perspective on brain network organization. Through analyses based on graph theory, large-scale brain network structures can be modeled using nodes at the voxel or regional level and structural or functional connections as edges (He & Evans, 2010). In this context, a graph can be defined as an abstract network model consisting of nodes and the edges connecting them (Bullmore & Sporns, 2012).

In a study based on structural MRI data, Liu et al. (2015) reported that children diagnosed with dyslexia exhibited increased local efficiency and a trend toward decreased global efficiency in gray matter structural networks compared to typically developing peers. Hosseini et al. (2013) analyzed structural connectivity derived from cortical surface area and found altered network topology in children at familial risk for reading difficulties, particularly indicating reduced connectivity in the left supramarginal gyrus and the left inferior frontal gyrus. In studies investigating functional brain network organization in dyslexia, EEG-based measurements have generally been preferred over fMRI (Vourkas et al., 2011; Finn et al., 2014; González et al., 2016). Finn et al. (2014) identified atypical functional connectivity in individuals with dyslexia both within the visual processing pathways and between visual

association areas and prefrontal attention networks. González et al. (2016) reported that, during rest, children with dyslexia demonstrated lower network integration across nodes in the theta frequency band compared to typically developing children. In another EEG study by Vourkas et al. (2011), children with dyslexia showed significantly reduced global efficiency in the alpha and gamma bands, as well as decreased local efficiency in the alpha band, during a phonological decoding task.

In studies investigating the topological properties of the brain in dyslexia using fMRI, Yang & Tan. (2020), concluded that children with dyslexia have less integrated brain networks and more modular organization. In their study, Zhang et al. (2021) found that the dyslexia group had higher local efficiency and clustering coefficient values compared to the typically developing group. Liu et al. (2016) found higher local efficiency and modularity in children with reading difficulties. They concluded that the brain network organization of children who have difficulty reading in a second language functions differently and that these children have lower cognitive flexibility. Zhang et al. (2021) demonstrated that subcortical regions, including the right putamen and left pallidum, play a pivotal role in the network topology of typically developing children, while showing altered nodal degree in dyslexic readers.

Recent functional neuroimaging studies have increasingly conceptualized developmental dyslexia not merely as a localized deficit in language areas, but as a topological aberration in large-scale brain network organization. Contemporary graph-theoretical literature indicates reduced global integration and altered regional efficiency during information processing in dyslexic individuals. Consequently, the investigation of nodal graph metrics, such as degree centrality and nodal efficiency, offers significant potential as clinical biomarkers for identifying neural phenotypes of dyslexia and mapping the neuroplastic changes induced by specialized educational interventions. However, studies directly contrasting the network topology of treatment-naïve, newly diagnosed children with dyslexia against their specially educated peers remain scarce in the literature.

In this study, graph theory-based analyses were performed on resting-state and continuous reading task fMRI data obtained from an initial diagnosis dyslexia group, educated children with dyslexia group, and a control group. Unlike the focus of most studies in the literature, this study also examined the educated children with dyslexia group, and analyses and comparisons were conducted for all groups under both resting state and reading task conditions. Within the scope of the study, brain networks that emerged during rest and reading tasks were first compared to examine the effect of different cognitive states on network organization. Then, inter-group comparisons were made, and within-group relationships between graph metrics were evaluated through correlation analyses. In this way, it was aimed to reveal how dyslexia-specific potential connectivity differences change in both task and resting conditions.

MATERIALS AND METHODS

Participants

This study included a total of 74 children: 25 diagnosed with dyslexia (Dys) according to DSM-V criteria (American Psychiatric Association [APA], 2013), 24 with a history of special education and no other psychiatric disorders (EDys) (Turgut Turan et al., 2016), and 25 healthy (HC). An individualized education program was applied for each child who received education (Ministry of National Education, n.d.). The native language of all children is Turkish. For the individuals receiving special education included in the study, an Individualized Education Program (IEP) was implemented for 12-24 months, prepared following the guidelines of the Ministry of National Education (MEB). This program was systematically structured according to the individual development and learning needs of the student (see https://orgm.meb.gov.tr/meb_iys_dosyalar/2025_03/13111054_21130110_ogrenme_guclugu.pdf). The participants were selected from individuals who had an MEB-approved Children's

Special Needs Report (ÇÖZGER) that officially documents their receipt of special education support. Thus, the special education process was based on both legal and pedagogical foundations. The demographic information of the participants is presented in Table 1. The study was conducted with the approval of XXXX University Ethics Committee (Decision No: XXXX), and written informed consent was obtained.

Table 1. Demographic informations and performance values

	Dys	EDys	HC	p values
Number of participants (N)	25	24	25	-
Gender (F/M)	8/17	9/15	12/13	0.533
Age (mean ± SD)	8,68 ± 1,51	9,62 ± 1,40	9,84 ± 1,57	0,022*
Duration of receiving special education (month) (mean ± SD)	-	16,25 ± 9,10	-	-
Other parameters: Participants consisted of Turkish-speaking children aged between 7 and 12 years with an IQ above 80, who met the diagnostic criteria according to DSM-V. In the educational group, the duration of the educational program ranged between 12 and 24 months. ANOVA test post hoc TUKEY HSD (*Dys vs HC)				

Data Acquisition

Structural and functional magnetic resonance images of each participant were acquired at the Department of Pediatric Radiology, XXXX University, using a Siemens Magnetom Aera 1.5 Tesla MRI device equipped with a 20-channel head coil.

Structural Imaging

Structural brain images were obtained using the T1-weighted MPRAGE (Magnetization-Prepared Rapid Gradient Echo) sequence. The scans were performed in the sagittal plane with the following parameters: echo time (TE) = 2.670 ms, repetition time (TR) = 1900 ms, matrix size = 256 × 256, isotropic resolution = 1.3 mm, and flip angle = 15°. A total of 192 slices were scanned, and the entire process took approximately 4 minutes and 18 seconds.

Functional Imaging

Functional magnetic resonance images were obtained using a T2-weighted echo-planar imaging (EPI) sequence. The scan parameters were as follows: TR = 2800 ms, TE = 53 ms, flip angle = 90°, field of view (FOV) = 192 mm, number of slices = 25, slice thickness = 5 mm, and in-plane resolution = 2 × 2 mm. Two separate fMRI sessions were conducted for each participant: one during the resting state and the other during a reading task. Each session lasted approximately 6 minutes and 14 seconds, yielding 130 image volumes (Gengeç Benli et al., 2024).

Experimental Design

Prior to data acquisition, written informed consent was obtained from the parents or legal guardians of all participating children. Additionally, verbal and written assent was explicitly obtained from the children themselves after they were fully informed about the study procedures in an age-appropriate manner.

Prior to the resting-state fMRI (rs-fMRI) acquisition, a high-resolution T1-weighted anatomical scan was performed as a standard acquisition sequence. During the preprocessing stage, these structural T1 images were utilized as a reference anatomy onto which the functional fMRI images were co-registered and aligned. During the resting-state scan, participants were instructed to keep their eyes open, relax, and allow their minds to wander freely without focusing on any particular topic. An observer was present in the scanner room throughout the imaging sessions to closely monitor the participants and ensure their adherence to the resting-state instructions. Directly following this, in the reading task scan, they were asked to silently

read a Turkish text appropriate for their age level (Ministry of National Education, n.d.). Unlike the frequently used stop-start model in the literature, a continuous reading model was applied in the reading task. To ensure participants task compliance, engagement, and alertness during both the resting-state and reading-task conditions, a designated observer was present in the scanner room throughout all imaging sessions to closely monitor the participants eye movements. Furthermore, to verify cognitive engagement and text comprehension during the continuous silent-reading paradigm, participants were administered a set of comprehension questions regarding the narrative immediately after exiting the scanner.

Data Preprocessing

Functional data were preprocessed using the FSL software (Smith et al., 2004). The preprocessing steps included brain extraction using BET, motion correction using MCFLIRT, slice timing correction (Parker, Liu, & Razlighi, 2017), Gaussian smoothing (FWHM = 5 mm), motion artifact removal using ICA-AROMA, high-pass filtering (cut-off = 0.01 Hz), and alignment to anatomical images (Smith et al., 2013). Participants with head motion exceeding 2 mm/° or average motion exceeding 0.5 mm/° were excluded (Sörös et al., 2019; Winkler et al., 2014). Images were normalized to the MNI152 template.

Network Analysis

All graph analyses in this study were conducted using the Graph Theoretical Network Analysis (GRETNA) toolbox, developed by Wang et al. (2015). Using the AAL-116 atlas, the brain was divided into 116 regions, and correlation matrices were created by calculating Pearson correlation coefficients (Tzourio-Mazoyer et al., 2002). After Fisher z-transformation, thresholded binary networks were obtained. In the analysis, nodal metrics calculated by AUC values (degree centrality, betweenness centrality nodal efficiency, nodal local efficiency, nodal clustering coefficient) were used. Each nodal graph metric was estimated exactly once per participant per condition (one unified network for the resting-state run and one for the reading task run); no repeated runs or split-session iterations were performed.
In this way, differences between nodal metrics during resting state and reading task within each group were examined.

Statistical Analysis

The assumption of normality was assessed using the Shapiro-Wilk test in SPSS version 27. Parametric t-tests were conducted for data exhibiting normal distribution, whereas non-parametric Mann-Whitney U tests were applied to data that did not meet the normality assumption. These analyses were performed separately for the Dys, EDys, and HC groups. Statistically significant differences in graph metrics were evaluated at a significance threshold of $p < 0.05$.

Additionally, the correlations between each metric across the groups were examined. Within each group, correlations between the metrics were analyzed. Pearson correlation was used for normally distributed data, while Spearman correlation was used for non-normally distributed data.

RESULTS

In this study, nodal metrics computed through graph analysis using the GRETNA toolbox were evaluated to compare resting-state and reading conditions in the fMRI data of the Dys, EDys, and HC groups. These metrics include betweenness centrality (BC), degree centrality (DC), nodal efficiency (NE), nodal local efficiency (NLE), and nodal clustering coefficient (NCC).

Comparison of Graph Metrics Between Conditions

The results of the node regions showing significant differences between conditions for the five nodal metrics in the Dys, EDys, and HC groups are presented in Table 2 and Figure 1.

According to Table 2, graph analysis revealed that in the Dys group, higher values were obtained in the reading task compared to the resting state for BC, DC, and NE metrics in the right superior frontal gyrus (R SFG) and right superior parietal lobe (R SPL). In contrast, higher values were found during the resting state compared to the reading task for NLE and NCC metrics in the left rectus, right rectus, and right cerebellum regions. In the left superior temporal gyrus (L STG), DC and NE metrics showed higher values in the resting state compared to the reading task.

In the EDys group, the right superior temporal pole (R STP) and left angular gyrus showed higher BC and DC values during the resting state compared to the reading task, while the left precentral gyrus, right postcentral gyrus, and right posterior cingulate showed higher NLE and NCC values during resting state relative to the reading task. Conversely, the left inferior occipital gyrus (L IOG) showed higher DC and NE values during the reading task compared to the resting state.

In the HC group, higher values were found in the resting state compared to the reading task for BC and NCC metrics in the left fusiform gyrus, and for NLE and NCC metrics in the right calcarine cortex and right Heschl's gyrus.

Table 2. Comparison of nodal metrics between resting-state and reading task

Betweenness Centrality				
	Anatomical Region	**Difference between groups**	**t value**	**p value**
Dys	L IFG (orb), R Hippocampus, R fusiform	RS>RT	-2.163, 2.351, 2.133	0.031, 0.024, 0.040
	R SFG, L STPole	RT>RS	-2.380, -2.297	0.022, 0.027
EDys	L Parahipocampal, L Angular gyrus, R STP	RS>RT	2.401, 2.518, 2.476	0.022, 0.016, 0.019
	L IOG, R Postcentral gyrus, L Paracentral lob, R Caudate nucleus	RT>RS	-2.268, -2.346, -2.098, -3.710	0.023, 0.023, 0.041, <0.001
HC	R Suplamantary motor area	RS>RT	2.096	0.043
	L Fusiform gyrus, L Putamen	RT>RS	-2.241, -3.276	0.025, 0.002
Degree Centrality				
	Anatomical Region	**Difference between groups**	**t value**	**p value**
Dys	R Olfactory Cortex, L STG	RS>RT	2.369, 2.457	0.023, 0.018
	R SFG, R SPL	RT>RS	-2.018, -2.114	0.044, 0.040
EDys	L MFG, L Angular gyrus, R STP	RS>RT	2.028, 2.157, 2.568	0.048, 0.036, 0.014
	L IOG	RT>RS	-3.088	0.003
Nodal Efficiency				
	Anatomical Region	**Difference between groups**	**t value**	**p value**
Dys	L STG	RS>RT	2.570	0.013
	R SFG, R SPL	RT>RS	-1.970, -2.066	0.049, 0.040
EDys	R Post Cingulate gyrus, R STP	RS>RT	2.087	0.042,0.037
	R MFG, L MOG, L IOG, R Caudate nucleus	RT>RS	-2.605, -2.048, -2.746, -2.165	0.009,0.046, 0.006,0.036
HC	L SFG, R Hippocampus,	RT>RS	-2.366, -2.302,	0.018, 0.021, 0.040

	L Caudate Nucleus		-2.109	
Nodal Local Efficiency				
	Anatomical Region	**Difference between groups**	**t value**	**p value**
Dys	L Rectus, R Rectus R Cerebellum (4,5)	RS>RT	2.701, 2.513, 2.638	0.010, 0.015, 0.011
	R Middle Cingulate gyrus	RT>RS	-2.022	0.043
EDys	L Precentral, L IFG (orb), R Posterior Cingulate, L Postcentral, R Postcentral	RS>RT	2.426, 2.248, 2.239, 2.020, 2.446	0.019, 0.029,0.030, 0.049, 0.018
	R ITG	RT>RS	-1.987	0.047
HC	R Calcarine Cortex R Heschl gyrus, L STG	RS>RT	2.326, -3.171, -2.038	0.024, 0.002, 0.042
Nodal Cluster Coefficient				
	Anatomical Region	**Difference between groups**	**t value**	**p value**
Dys	L MFG (orb), L Rectus, R Rectus	RS>RT	2.042, 2.494, 2.087	0.047, 0.016, 0.042
	L Cerebellum crus 2, R Cerebellum (4,5), Vermis 6	RS>RT	2.160, 2.139, 2.051	0.036, 0.038, 0.046
EDys	L Precentral gyrus, R Posterior Cingulate gyrus	RS>RT	2.065, 2.394	0.045, 0.021
	R Postcentral gyrus, L Cerebellum (lob10), Vermis 10	RS>RT	2.814, 2.148, 2.275	0.007, 0.037, 0.028
HC	R Posterior Cingulate gyrus, L Amygdala, R Calcarine	RS>RT	2.181, 2.272, 2.301	0.035, 0.028, 0.026
	L Fusiform gyrus, R Helschl gyrus, Vermis 10	RS>RT	2.021, 2.817, -2.070	0.049, 0.007, 0.038

RS: Resting-state, RT: Reading-task

Quantitative network analysis revealed that the magnitude of topological alterations varied distinctively across regions. The most pronounced localized difference between the reading task and resting state was observed in the right superior frontal gyrus for degree centrality (DC) within the Dys group, which exhibited the highest statistical significance ($t = 2.74$, $p < 0.05$). Conversely, the smallest significant topological change was detected in the left inferior occipital gyrus for nodal efficiency (NE) within the EDys cohort ($t = 2.02$, $p<0.05$). The metrics in which these network changes were most prominently observed across all participants were Degree Centrality (DC) and Nodal Efficiency (NE).

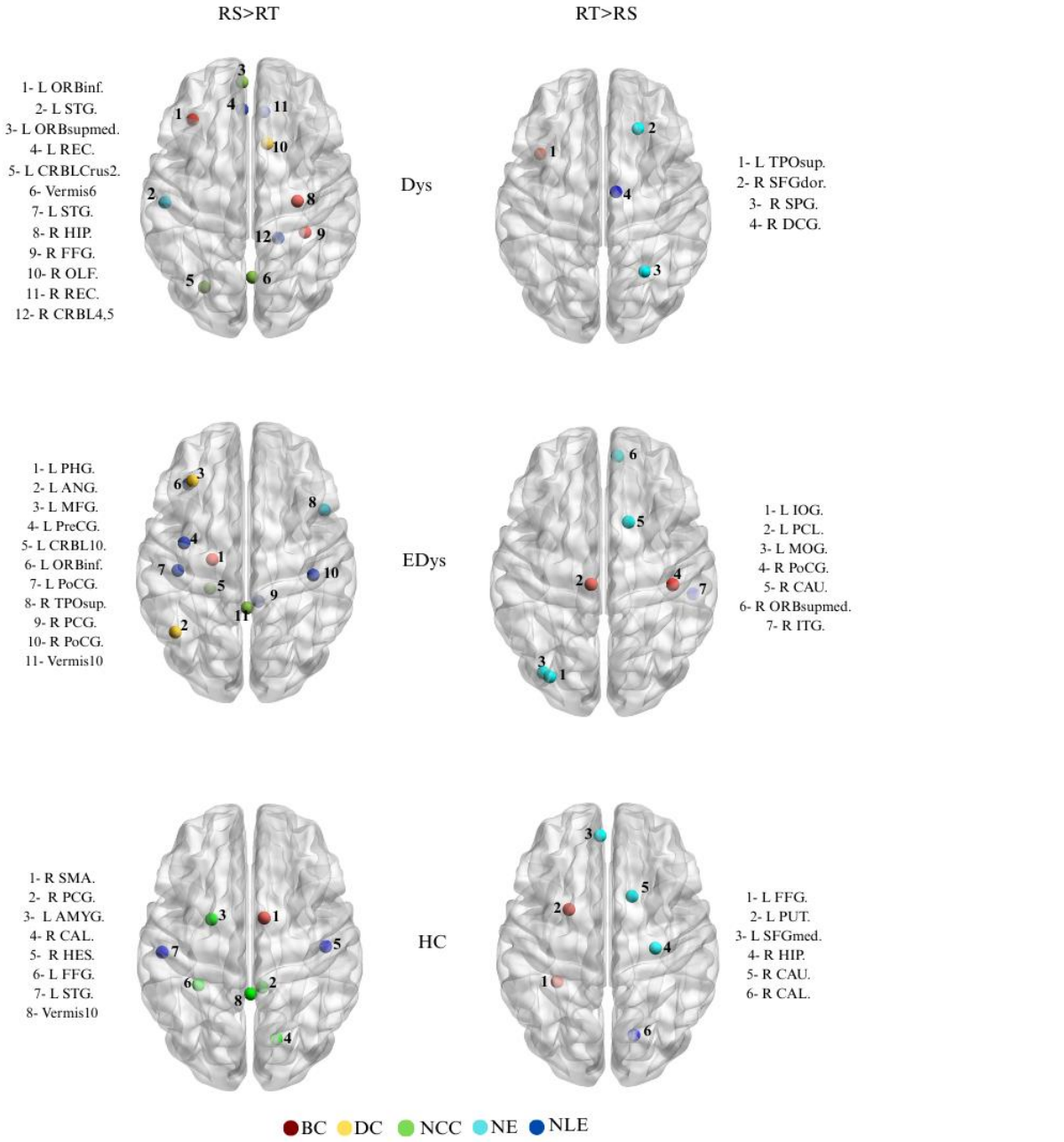

Figure 1. Brain regions exhibiting statistically significant differences between network states ($p < 0.05$). The spheres represent the specific brain regions showing topological alterations between the resting state (RS) and the reading task (RT). Each examined graph metric is assigned a distinct color

Correlation Analysis Results

Based on the results of the graph analysis, correlation analyses were conducted both between the groups and within each group for the obtained nodal metrics. According to the intergroup correlation analysis results, only the regions with an absolute correlation value greater than 0.5 were included. In Table 3, the number of regions showing intergroup correlations for each relevant metric is provided, allowing comparison based on the abundance or scarcity of correlated brain regions across metrics.

Between the Dys and HC groups, during the resting-state the highest number of correlated regions was observed in the BC metric, followed by the NE metric, while no correlations were found in the other metrics. During the reading task, more correlated regions were found between the Dys and HC groups in the NE, DC, and BC metrics, respectively. Between the Dys and EDys groups, during the resting-state correlations were found in more metrics but fewer

regions, and no correlated regions were observed for the NCC metric. During the reading task, fewer correlations were observed overall, and no correlations were found in the BC and DC metrics. Between the EDys and HC groups, during the resting-state again, no correlation was observed only in the NCC metric. During the reading task, correlations were found in all metrics, with the highest number of correlated regions observed in the NLE, DC and NCC metrics.

Table 3. Correlation results between groups

Metric/group	**Dys-HC**		**Dys-EDys**		**EDys-HC**	
	RS	RT	RS	RT	RS	RT
BC	5	2	2	-	1	1
DC	-	4	1	-	2	5
NE	2	5	2	2	1	2
NLE	-	-	1	1	2	7
NCC	-	-	-	1	-	5

The results of nodal regions with correlation coefficients above an absolute value of 0.7 among metrics within each group are presented in Table 4 and Table 5. An examination of Table 4 shows that during the resting state, almost all regions exhibited correlations between DC and NE across all groups. Additionally, correlations between BC and NE, followed by BC and DC, were higher in all groups. An examination of Table 5 shows that during the reading task, the relationships between DC, BC, and NE were similar to those observed in the resting state. For the NCC and BC metrics, correlations were approximately similar in the EDys and HC groups, whereas the Dys group showed lower correlations. Similarly, the pattern of correlations between NLE and BC was approximately comparable in the EDys and HC groups but lower in the Dys group.

Table 4. Resting state correlation results of Dys, EDys and HC groups

	Metrics	BC	DC	NE	NLE	NCC
Dys	BC		41	49	8	10
	DC	41		116	3	3
	NE	49	116		8	3
	NLE	8	3	8		115
	NCC	10	3	3	115	
EDys	BC		40	47	5	7
	DC	40		116	14	6
	NE	47	116		12	4
	NLE	5	14	12		116
	NCC	7	6	4	116	
HC	BC		20	37	8	12
	DC	20		111	22	16
	NE	37	111		20	14
	NLE	8	22	20		116
	NCC	12	16	14	116	

Table 5. Reading task correlation results of Dys, EDys and HC groups

	Metrics	BC	DC	NE	NLE	NCC
Dys	BC		37	42	4	2
	DC	37		116	10	4
	NE	42	116		10	3
	NLE	4	10	10		116
	NCC	2	4	3	116	
EDys	BC		28	35	8	13
	DC	28		116	8	3
	NE	35	116		9	3
	NLE	8	8	9		114
	NCC	13	3	3	114	
HC	BC		31	47	11	14
	DC	31		112	14	6
	NE	47	112		12	5
	NLE	11	14	12		115
	NCC	14	6	5	115	

DISCUSSION

In this study, fMRI data from child participants in the Dys, EDys, and HC groups were examined through graph analysis metrics to investigate brain network connectivity during resting state and reading task. Analyses conducted using betweenness centrality (BC), degree centrality (DC), nodal efficiency (NE), nodal local efficiency (NLE), and nodal clustering coefficient (NCC) metrics revealed differences in correlations both between conditions and among groups.

In the Dys group, the higher BC, DC, and NE values in the R SFG and R SPL regions during the reading task compared to the resting state suggest that these regions are associated with increased information exchange and network integration during reading (Schurz et al., 2014). Similar differences in brain network connectivity related to dyslexia have been reported in the literature. Schurz et al. reported reduced connectivity between the left posterior temporal regions and the left inferior frontal gyrus in individuals diagnosed with dyslexia during both task performance and resting state (Schurz et al., 2014). The higher NLE and NCC values observed in the Dys group in the L rectus, R rectus, and R cerebellum regions during the resting state indicate that these areas exhibit stronger local connectivity when the brain is not engaged in a task (Finn et al., 2014).

In the EDys group, higher BC and DC values in the R STP and L angular gyrus during resting state compared to the reading task suggest that these regions act as more critical hubs during the off-task period. Additionally, increased NLE and NCC values in the L precentral gyrus, R postcentral gyrus, and R postcingulate during resting state may reflect enhanced local connectivity in motor and attention-related regions following training in these individuals (Koyama et al., 2013). Furthermore, increased DC and NE values in the L IOG during the reading task compared to rest may reflect the contribution of this region to visual processing (Dehaene et al., 2010). In the study by Koyama et al., decreased connectivity between the left intraparietal sulcus and the left fusiform gyrus was reported in children diagnosed with dyslexia; however, following reading training, this connectivity was enhanced, along with increased connections to the right middle occipital gyrus. These findings highlight the potential of training to reorganize brain network connectivity. (Koyama et al., 2013).

In the HC group, higher BC and NCC metrics in the left fusiform gyrus and higher NLE and NCC metrics in the right calcarine cortex and right Heschl's gyrus during resting state suggest that these regions demonstrate strong local connectivity and information flow during the off-task period in typically developing individuals (Bitan et al., 2007). Considering the fusiform gyrus is linked to visual word recognition, these results support the notion that these areas are more effectively organized in typical development (Bitan et al., 2007).

When examining the correlations of nodal metrics between groups during the reading task, correlations were observed across all metrics in the EDys and HC groups. This finding indicates that dyslexic children who have received training exhibit network organization similar to that of healthy individuals during reading. This suggests that education positively influences network organization in dyslexia and supports more efficient information processing during reading.

Looking at correlations among metrics within each group during the resting state, the Dys and EDys groups showed correlations between BC and DC as well as between BC and NE in a greater number of nodal regions compared to the HC group. This suggests that in Dys and EDys groups, central nodes engage more extensively in information flow and network integration (Fraga et al., 2016).

In the HC group, the number of correlations between NCC and the BC, DC, and NE metrics during rest was higher than in the Dys and EDys groups. This finding indicates that in healthy individuals, local clustering properties are better integrated with central nodes, resulting in more efficient network organization (Fraga et al., 2018).

CONCLUSION

In conclusion, our findings demonstrate that developmental dyslexia involves a broad alteration in brain network organization that extends beyond the functional reading process. Rather than non-specific trends, our localized evaluations show that structured special education drives a targeted topological normalization. Specifically, the educated dyslexia (EDys) group exhibited a clear structural convergence toward healthy control (HC) configurations within left-hemisphere integration hubs. This was explicitly driven by a robust alignment in Betweenness Centrality (BC) within the left angular gyrus and active Degree Centrality (DC) within the left inferior occipital gyrus, where the magnitude of statistical difference between EDys and HC was rendered non-significant ($p > 0.05$)

Looking ahead, these whole-brain graph-theoretical metric profiles hold great potential as fMRI-based biomarkers for the objective diagnosis of dyslexia and the quantification of treatment response.

Limitations

A primary limitation of this study is the lack of strict age matching across the participant groups. Because the 7–12 age range is characterized by rapid neurodevelopmental maturation, it is possible that some variations in graph metrics were partially influenced by age variance. However, clinical challenges in recruiting treatment-naïve dyslexic children (Dys) and those with specific special education backgrounds (EDys) rendered this age variation unavoidable during sampling. Future studies utilizing narrower and precisely matched age cohorts are warranted to fully dissociate general neurodevelopmental maturation from dyslexia-specific network reconfigurations. Another technical limitation of this study is that fMRI data were acquired using a 1.5 Tesla scanner with a 5 mm slice thickness. Compared to current 3T imaging standards, 1.5T systems offer lower spatial resolution and a reduced signal-to-noise ratio (SNR). This constraint may have limited the spatial specificity of the graph metrics, particularly within smaller or closely adjacent brain regions. Future studies utilizing higher field strengths (3T or higher) and high-resolution protocols are warranted to map these topological alterations

with greater precision. Another limitation is the absence of an a priori power analysis to determine the sample size (Dys=25, EDys=24, HC=25). The cohort size was constrained by the clinical difficulties of recruiting specific pediatric populations and was based on comparable fMRI studies in the literature. This constraint may have limited the statistical power, potentially affecting the detection of subtle network alterations. Future studies with larger sample sizes are warranted to achieve higher statistical power and improve the generalizability of the findings.

Acknowledgements: We would like to thank to Expert Psychiatrist Dr. Büşra Sertkaya, and Erciyes University Pediatric Radiology Department, MR Technician Tuğba Özalp, and Ünal Şahinci for data acquisition.

Funding Statement: This study was supported by the Scientific and Technological Research Council of Türkiye (TÜBİTAK) under project number 122E131. The authors thank to TÜBİTAK for their supports.

Data Availability Statement: This study is carried out within the scope of the TÜBİTAK project and data sharing cannot be done yet.

Conflict of Interest disclosure: The authors declare that there is no conflict of interest regarding the publication of this article.

Ethics Approval Statement: This study has been approved by the Erciyes University Clinical Research Ethics Committee (Decision No:2022/504).

Author Contributions

Plan, design: GRS, Sİ, ŞGB; **Material, methods and data collection:** GRS, Sİ, ŞGB, ED, ZFK; **Data analysis and comments:** GRS, Sİ, ŞGB, ED; **Writing and corrections:** GRS, Sİ, ŞGB.

REFERENCES

American Psychiatric Association. (2013). Diagnostic and statistical manual of mental disorders (5th ed.). American Psychiatric Publishing.

Bitan, T., Cheon, J., Lu, D., Burman, D. D., & Booth, J. R. (2007). Developmental changes in activation and effective connectivity in phonological and orthographic processing. NeuroImage, 38(3), 564–575.

Boets, B., Op de Beeck, H. P., Vandermosten, M., Scott, S. K., Gillebert, C. R., Mantini, D., ... & Ghesquière, P. (2013). Intact but less accessible phonetic representations in adults with dyslexia. Science, 342(6163), 1251–1254.

Bullmore, E., & Sporns, O. (2009). Complex brain networks: Graph theoretical analysis of structural and functional systems. Nature Reviews Neuroscience, 10(3), 186–198. https://doi.org/10.1038/nrn2575

Bullmore, E., & Sporns, O. (2012). The economy of brain network organization. Nature Reviews Neuroscience, 13(5), 336–349.

Dehaene, S., Pegado, F., Braga, L. W., Ventura, P., Nunes Filho, G., Jobert, A., ... & Cohen, L. (2010). How learning to read changes the cortical networks for vision and language. Science, 330(6009), 1359–1364.

Finn, E. S., Shen, X., Holahan, J. M., Scheinost, D., Lacadie, C., Papademetris, X., & Constable, R. T. (2014). Disruption of functional networks in dyslexia: A whole-brain, data-driven analysis of connectivity. Biological Psychiatry, 76(5), 397–404.

Fraga González, G., Van der Molen, M. J. W., Žarić, G., Bonte, M., Tijms, J., Blomert, L., ... & Van der Molen, M. W. (2016). Graph analysis of EEG resting state functional networks in dyslexic readers. Clinical Neurophysiology, 127(9), 3165–3175.

Fraga González, G., Smit, D. J. A., van der Molen, M. J. W., Tijms, J., Stam, C. J., de Geus, E. J. C., & van der Molen, M. W. (2018). EEG resting state functional connectivity in adult dyslexics using phase lag index and graph analysis. Frontiers in Human Neuroscience, 12, 341.

Gengeç Benli, Ş., İçer, S., Demirci, E., Karaman, Z. F., Ak, Z., Acer, İ., ... & Sertkaya, B. (2024). Data-driven exploratory method investigation on the effect of dyslexia education at brain connectivity in Turkish children: A preliminary study. Brain Structure and Function.

He, Y., & Evans, A. (2010). Graph theoretical modeling of brain connectivity. Current Opinion in Neurology, 23(4), 341–350.

Hosseini, S. H., Black, J. M., Soriano, T., Bugescu, N., Martinez, R., Raman, M. M., ... & Hoeft, F. (2013). Topological properties of large-scale structural brain networks in children with familial risk for reading difficulties. NeuroImage, 71, 260–274.

Icer, S., Benli, S. G., Gumus, K., Demirci, E., Ozmen, S., & Doganay, S. (2018). Can functional connectivity at resting brain in ADHD indicate the impairments in sensory-motor functions and face/emotion recognition? Journal of Medical and Biological Engineering, 38(1), 138–149.

Koyama, M. S., Di Martino, A., Kelly, C., Jutagir, D. R., Sunshine, J., Schwartz, S. J., ... & Milham, M. P. (2013). Cortical signatures of dyslexia and remediation: An intrinsic functional connectivity approach. PLoS ONE, 8(2), e55454.

Liu, K., Shi, L., Chen, F., Waye, M. M., Lim, C. K., Cheng, P. W., ... & Wang, D. (2015). Altered topological organization of brain structural network in Chinese children with developmental dyslexia. Neuroscience Letters, 589, 169–175.

Liu, L., Li, H., Zhang, M., Wang, Z., Wei, N., Liu, L., ... & Ding, G. (2016). Aberrant topologies and reconfiguration pattern of functional brain network in children with second language reading impairment. Developmental Science, 19(4), 657–672.

Lyon, G. R., Shaywitz, S. E., & Shaywitz, B. A. (2003). A definition of dyslexia. Annals of Dyslexia, 53, 1–14.

Norton, E. S., Beach, S. D., & Gabrieli, J. D. (2015). Neurobiology of dyslexia. Current Opinion in Neurobiology, 30, 73–78.

Oğrenme güçlüğü olan bireyler için destek eğitim programı. (n.d.). Türkiye Cumhuriyeti Millî Eğitim Bakanlığı. https://orgm.meb.gov.tr/

Parker, D., Liu, X., & Razlighi, Q. R. (2017). Optimal slice timing correction and its interaction with fMRI parameters and artifacts. Medical Image Analysis, 35, 434–445.

Schurz, M., Wimmer, H., Richlan, F., Ludersdorfer, P., Klackl, J., & Kronbichler, M. (2014). Resting-state and task-based functional brain connectivity in developmental dyslexia. Cerebral Cortex, 24(9), 2654–2661.

Smith, S. M., Jenkinson, M., Woolrich, M. W., Beckmann, C. F., Behrens, T. E., Johansen-Berg, H., ... & Matthews, P. M. (2004). Advances in functional and structural MR image analysis and implementation as FSL. NeuroImage, 23(S1), 208–219.

Sörös, P., Hoxhaj, E., Borel, P., Sadohara, C., Feige, B., Matthies, S., et al. (2019). Hyperactivity / restlessness is associated with increased functional connectivity in adults with ADHD: A dimensional analysis of resting state fMRI. NeuroImage: Clinical, 21, 1–11.

Turgut Turan, S., Erdoğan Bakar, E., Erden, G., & Karakaş, S. (2016). Using neuropsychometric measurements in the differential diagnosis of specific learning disability. Noro Psikiyatri Arsivi, 53(2), 144–151.

Tzourio-Mazoyer, N., Landeau, B., Papathanassiou, D., Crivello, F., Etard, O., Delcroix, N., ... & Joliot, M. (2002). Automated anatomical labeling of activations in SPM using a macroscopic anatomical parcellation of the MNI MRI single-subject brain. NeuroImage, 15(1), 273–289.

van der Mark, S., Klaver, P., Bucher, K., Maurer, U., Schulz, E., Brem, S., ... & Brandeis, D. (2011). The left occipitotemporal system in reading: Disruption of focal fMRI connectivity to left inferior frontal and inferior parietal language areas in children with dyslexia. NeuroImage, 54(3), 2426–2436.

Vandermosten, M., Boets, B., Wouters, J., & Ghesquière, P. (2012). A qualitative and quantitative review of diffusion tensor imaging studies in reading and dyslexia. Neuroscience & Biobehavioral Reviews, 36(6), 1532–1552.

Vogel, A. C., Miezin, F. M., Petersen, S. E., & Schlaggar, B. L. (2012). The putative visual word form area is functionally connected to the dorsal attention network. Cerebral Cortex, 22(3), 537–549.

Vourkas, M., Micheloyannis, S., Simos, P. G., Rezaie, R., Fletcher, J. M., Cirino, P. T., & Papanicolaou, A. C. (2011). Dynamic task-specific brain network connectivity in children with severe reading difficulties. Neuroscience Letters, 488(2), 123–128.

Wang, J., Wang, X., Xia, M., Liao, X., Evans, A., & He, Y. (2015). GRETNA: A graph theoretical network analysis toolbox for imaging connectomics. Frontiers in Human Neuroscience, 9, 386.

Winkler, A. M., Ridgway, G. R., Webster, M. A., Smith, S. M., & Nichols, T. E. (2014). Permutation inference for the general linear model. NeuroImage, 92, 381–397.

Yang, J., & Tan, L. H. (2020). Whole-brain functional networks for phonological and orthographic processing in Chinese good and poor readers. Frontiers in Psychology, 10, 2945.

Zhang, L., Hu, J., Liu, X., Nichols, E. S., Lu, C., & Liu, L. (2021). Disrupted subcortical-cortical connections in a phonological but not semantic task in Chinese children with dyslexia. *Frontiers in Human Neuroscience, 14*, Article 611008.

Zhang, J., Liu, L., Li, H., Feng, X., Zhang, M., Liu, L., ... & Ding, G. (2021). Large-scale network topology reveals brain functional abnormality in Chinese dyslexic children. Neuropsychologia, 157, 107886.